

# Nitrile Imines: Matrix Isolation, IR Spectra, Structures, and Rearrangement to Carbodiimides

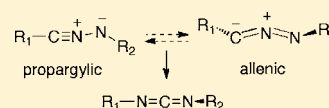
Didier Bégué,<sup>†</sup> Greg GuangHua Qiao,<sup>‡</sup> and Curt Wentrup<sup>\*,‡</sup>

<sup>†</sup>Institut Pluridisciplinaire de Recherche sur l'Environnement et les Matériaux, Equipe Chimie Physique, UMR 5254, Université de Pau et des Pays de l'Adour, 64000 Pau, France

<sup>‡</sup>School of Chemistry and Molecular Biosciences, The University of Queensland, Brisbane, Queensland 4072, Australia

**S** Supporting Information

**ABSTRACT:** The structures and reactivities of nitrile imines are subjects of continuing debate. Several nitrile imines were generated photochemically or thermally and investigated by IR spectroscopy in Ar matrices at cryogenic temperatures (Ph-CNN-H **6**, Ph-CNN-CH<sub>3</sub> **17**, Ph-CNN-SiMe<sub>3</sub> **23**, Ph-CNN-Ph **29**, Ph<sub>3</sub>C-CNN-CPh<sub>3</sub> **34**, and the boryl-CNN-boryl derivative **39**). The effect of substituents on the structures and IR absorptions of nitrile imines was investigated computationally at the B3LYP/6-31G\* level. IR spectra were analyzed in terms of calculated anharmonic vibrational spectra and were generally in very good agreement with the calculated spectra. Infrared spectra were found to reflect the structures of nitrile imines accurately. Nitrile imines with IR absorptions above 2200 cm<sup>-1</sup> have essentially propargylic structures, possessing a CN triple bond (typically PhCNNSiMe<sub>3</sub> **23**, PhCNNPh **29**, and boryl-CNN-boryl **39**). Nitrile imines with IR absorptions below ca. 2200 cm<sup>-1</sup> are more likely to be allenic (e.g., HCNNH **1**, PhCNNH **6**, HCNPh **43**, PhCNNCH<sub>3</sub> **17**, and Ph<sub>3</sub>C-CNN-CPh<sub>3</sub> **34**). All nitrile imines isomerize to the corresponding carbodiimides both thermally and photochemically. Monosubstituted carbodiimides isomerize thermally to the corresponding cyanamides (e.g., Ph-N=C=N-H **5** → Ph-NH-CN **8**), which are therefore the thermal end products for nitrile imines of the types RCNNH and HCNNR. This tautomerization is reversible under flash vacuum thermolysis conditions.

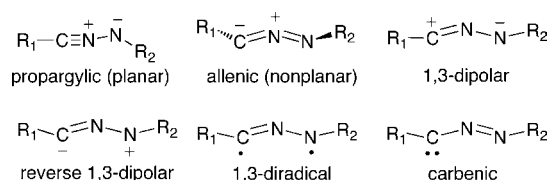


## INTRODUCTION

Nitrile imines are used widely in organic synthesis and in regioselective 1,3-dipolar cycloadditions leading to pyrazoles, pyrazolines, and many other compounds.<sup>1</sup> The structures and reactivities of nitrile imines are somewhat controversial subjects of ongoing debate.

Six alternative structures have been postulated for the nonstabilized nitrile imines: propargylic, allenic, 1,3-dipolar and reverse dipolar form, 1,3-diradical, and carbenic (Scheme 1). Of course, each individual molecule will have a particular

**Scheme 1. Six Fundamental Structures of Nitrile Imines**



structure, which may be closer to one of the six alternatives than the others. Each molecule can also be described by several canonical structures, which may have different weights. Theoretical calculations have yielded conflicting results. Early calculations indicated that the parent nitrilium betaines are floppy molecules, which may exist in either propargylic or allenic forms with low barriers between them.<sup>2</sup> High-level ab initio calculations with configuration interaction and large basis sets (QCISD/6-311+G(2df,2p)) concluded that the parent

nitrile imine has a nonplanar, allenic geometry, and that the propargylic structure is not a stable minimum on the HCNNH potential energy surface. In fact, all correlated methods were found to lower the energy of the allenic conformation relative to the propargylic one.<sup>3</sup> However, substituents can have a profound effect on the relative stabilities. Thus, bis(trityl)nitrile imine has been demonstrated to be allenic by X-ray crystallography, by diastereoselective cycloaddition in solution, and by calculation.<sup>4</sup>

DFT calculations in combination with the natural resonance theory suggested that four resonance structures are necessary for a full description (propargylic, allenic, 1,3-dipolar, and carbenic), and that the carbenic form dominates for F-CNN-F and H<sub>2</sub>N-CNN-NH<sub>2</sub>.<sup>5,6</sup> The carbenic forms would be stabilized by a neighboring lone pair. C<sub>2</sub>N-Diaminonitrile imine is predicted to be a stable carbene;<sup>7</sup> these aminocarbene forms would in fact have some of the character of the bent, zwitterionic, allenic form. In contrast, spin-coupled valence bond (VB) calculations using the geometry from a CASSCF-(8,6)/cc-pVTZ calculation denied the importance of the carbenic and allenic forms for the parent HCNNH and suggested that this molecule has a predominantly propargylic electronic structure albeit a bent, nonplanar, allenic-type geometry.<sup>8</sup>

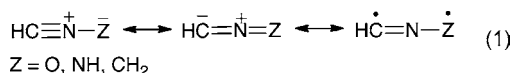
Ess and Houk have proposed a new model for 1,3-dipolar cycloaddition reactions, which decomposes the barrier into two

Received: December 20, 2011

Published: February 25, 2012

additive components: a distortion energy—that is, the energy required to distort the 1,3-dipole and to a much lesser extent the dipolarophile from their equilibrium geometries to the transition-state (TS) geometries—followed by an energy of interaction between the two distorted fragments at the TS. A remarkable correlation between barrier heights and distortion energies was found. Since the distortion involves bending of the dipole, the reaction should proceed more readily if the bending vibration is selectively excited.<sup>9</sup>

This model was further elaborated by Hiberty and co-workers, who studied a series of nine 1,3-dipoles, including the nitrilium betaines HCNZ (Z = O, NH, or CH<sub>2</sub>), by means of the breathing-orbital VB *ab initio* method. Here, each 1,3-dipole is described as a linear combination of three VB



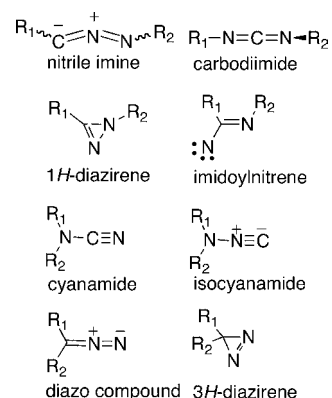
structures, two zwitterionic and one diradical (eq 1), for which the weights in the total wave function can be quantitatively estimated. The ground states of the nitrile imines were found to have approximately equal contributions from propargylic and allenic VB structures (38% and 36%, respectively), with a little less diradical character (26%), but the diradical characters of all nine dipoles studied was found to be a critical feature favoring 1,3-dipolar cycloaddition; a linear relationship was found between the weight of the diradical structure in the 1,3-dipole and the barrier to cycloaddition to ethylene or acetylene. The barrier heights also correlate very well with the transition energies from ground state to pure diradical states of the 1,3-dipoles at equilibrium geometry. Moreover, the weight of the diradical structure is shown to increase significantly in all 1,3-dipoles from their equilibrium geometries to their distorted geometries in the TSs. Thus it was proposed that the 1,3-dipole first distorts so as to reach a reactive state that possesses some critical diradical character and then adds to the dipolarophile with little or no barrier.<sup>10</sup>

Coppens et al. reported a direct X-ray crystallographic observation of a photogenerated, bent C,N-diarylnitrile imine structure in a Zn-coordinated crystal. The bent structure could be either the 1,3-dipolar (or 1,3-diradicaloid) or the carbenic form. Reaction with water resulted in addition of the OH group to C, thereby suggesting that the 1,3-dipolar form R<sup>1</sup>C<sup>+</sup>NN<sup>-</sup>R<sup>2</sup> or the carbenic form was a major electronic contributor.<sup>11</sup>

Although nitrile imines are not usually isolable under ordinary reaction conditions, several stable nitrile imines have been synthesized.<sup>12,13</sup> The main IR absorptions of the nitrile imine moiety can appear over a very wide frequency range, from 2000 to >2250 cm<sup>-1</sup>.<sup>12</sup> The parent nitrile imine HCNNH I absorbs at 2033 cm<sup>-1</sup> in Ar matrix,<sup>14</sup> whereas diphenylnitrile imine PhCNNPh absorbs at 2228 cm<sup>-1</sup> in PVC film.<sup>15</sup> As we will describe, DFT calculations match the experimental IR spectra of several stable and unstable nitrile imines very well. Therefore, it is reasonable to expect a correlation between the DFT-calculated structures and the IR spectra.

We will also show that nitrile imines are prone to rearrangement to the more stable carbodiimides. Rearrangement to diazo compounds has also been documented.<sup>12,16</sup> At least eight different structural isomers of nitrile imines need to be considered (Scheme 2). Experimental evidence for a nitrile imine–imidoylnitrene–carbodiimide rearrangement<sup>17,18</sup> and a 1*H*-azirine (isodiazirine)<sup>19</sup> has been reported.

## Scheme 2. Nitrile Imine Isomers



## RESULTS AND DISCUSSION

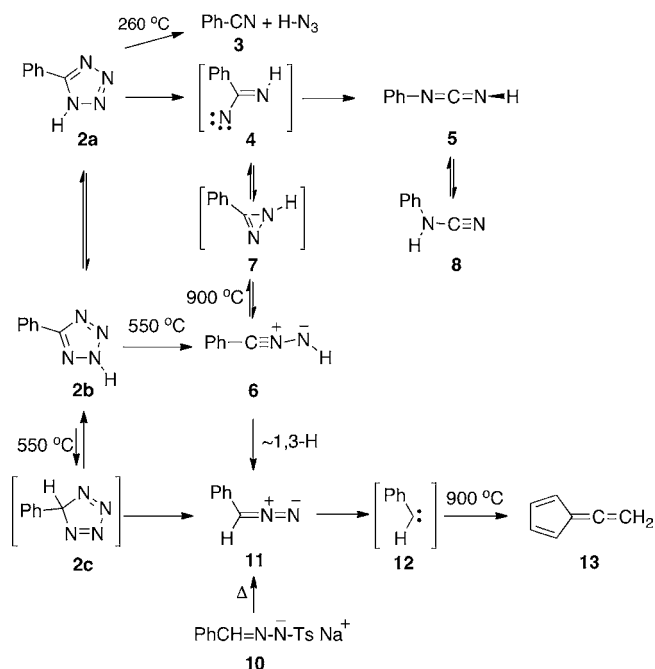
We have generated a variety of nitrile imines by either flash vacuum thermolysis (FVT) or matrix photolysis of tetrazoles and in one case also from an oxadiazolone. The thermal and photochemical reactions of the nitrile imines are described below, together with analyses of their observed and calculated IR spectra, which provide important information on the structures.

**C-Phenylnitrile Imine (Benzonitrile Imine 6).** Benzonitrile imine **6** has been invoked previously in thermolysis<sup>20,21</sup> and photolysis<sup>22</sup> reactions of 5-phenyltetrazole **2** in solution. Although **6** was not trappable by 1,3-dipolar cycloaddition reactions when generated photochemically, labeling experiments supported its intermediacy in the dimerization to dihydrotetrazines. Benzonitrile imine **6**, generated by thermolysis of 5-phenyltetrazole, was successfully trapped in 1,3-dipolar cycloaddition with nitriles.<sup>20</sup> C,N-Diarylnitrile imines are formed on thermolysis of 2,5-diaryltetrazoles in the gas phase and in solution.<sup>23</sup> It is instructive first to review the FVT reactions of 5-phenyltetrazole **2**, which will facilitate the characterization of some of the products formed in the matrix photolysis.

**Thermolysis of 5-Phenyltetrazole 2.** Deposition of 5-phenyltetrazole **2** in an Ar matrix at 12 K affords a ca. 2:1 mixture of the 1*H*- and 2*H*-tautomers **2a** and **2b**, as judged by comparison of the IR spectra with the calculated spectra at the B3LYP/6-31G\* level (see Supporting Information). Mild FVT of **2** at 260 °C with isolation of the products in Ar matrix gave rise to small amounts of HN<sub>3</sub> and benzonitrile **3**, formed by a retro-1,3-dipolar cycloaddition reaction<sup>24</sup> (Figure S1), as would be expected from the presence of the 1*H*-tetrazole tautomer **2a** in the gas phase (Scheme 3).

FVT of **2** at 550 °C afforded phenyldiazomethane **11** as a major product.<sup>24</sup> Figure S2 shows the Ar matrix IR spectra of **11** isolated from this thermolysis and from the benzaldehyde tosylhydrazone sodium salt **10**. The formation of **11** from **2** can occur via either of two mechanisms: (i) Elimination of nitrogen from **2b** forms nitrile imine **6**, which, under FVT conditions, can undergo a further 1,3-*H* shift to form diazo compound **11** (Scheme 3). Nitrile imine-to-diazo compound rearrangements have been postulated<sup>25</sup> and observed<sup>12</sup> in other experiments. (ii) A 1,5-*H* shift to give 5-phenyl-5*H*-tetrazole **2c** (Scheme 3) is an attractive alternative mechanism; elimination of nitrogen from **2c** would form diazo compound **11**. High-level *ab initio* calculations<sup>26</sup> indicated that the 5*H*-tetrazole is an experimentally accessible species. The isomerization barrier calcu-

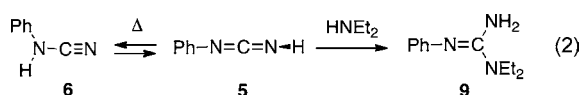
## Scheme 3. Thermolysis of 5-Phenyltetrazole



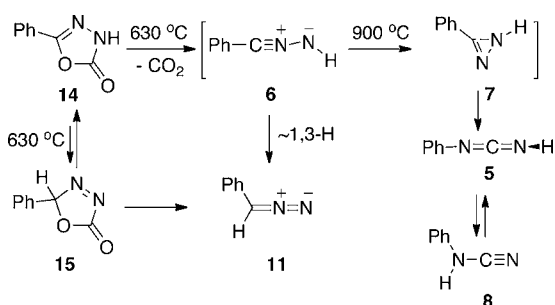
lated for the gas-phase 1,5-shift of H from N1 to N2 is 49 kcal/mol, and for the 1,5-shift of H from N1 to C5 it is 55 kcal/mol at the QCISD(T)/6-311+G(2d,2p) level.<sup>26</sup> These barriers are high, but potentially accessible under high-temperature FVT conditions.

On FVT of **2** at 900 °C, phenyldiazomethane was no longer observable. Instead, phenylcarbodiimide **5** (2128/2167  $\text{cm}^{-1}$ ) and phenylcyanamide **8** (2255/2236  $\text{cm}^{-1}$ ) were observed in the Ar matrix IR spectrum. In addition, an absorption at 1954  $\text{cm}^{-1}$  is ascribed to the rearrangement of phenylcarbene **12** to fulvenallene **13** (Scheme 3).<sup>27</sup> Carbodiimide **5** can arise from the 1*H*-tetrazole **2a** and/or rearrangement of the nitrile imine **6** (Scheme 3). The mechanism and the IR spectrum of **5** are described further below.

Compounds **5** and **8** were identified by direct comparison with authentic compounds. Phenylcarbodiimide **5** was obtained by FVT of phenylcyanamide **8** at 550 °C and characterized on the basis of its IR spectrum (Figure S3). Moreover, **5** was trapped with diethylamine at 77 K to furnish the guanidine **9** in 57% yield (eq 2).

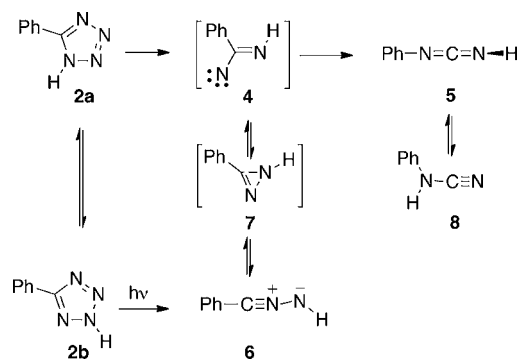
Thermolysis of 5-Phenyl-1,3,4-oxadiazol-2(3*H*)-one **14**.

Compound **14** was used as an alternate, potential precursor of nitrile imine **6** (Scheme 4). FVT was carried out in the 600–900 °C range with isolation of the products in Ar matrix at 12 K. At the lowest temperature, phenyldiazomethane **11** was again observed together with  $\text{CO}_2$ . The formation of **11** may be due to a 1,3-H shift in benzonitrile imine **6**, but a 1,3-H shift (or two consecutive 1,2-H shifts) of **14** to **15**, with subsequent elimination of  $\text{CO}_2$ , cannot be ruled out (Scheme 4). On FVT at 700–800 °C, less diazo compound **11** was obtained, and phenylcyanamide **8** was now formed together with phenylcarbodiimide **5**. At 900 °C, only **5**, **8**, and  $\text{CO}_2$  were isolated (Figure S4). Since phenyldiazomethane does not isomerize

Scheme 4. Thermolysis of 5-Phenyl-1,3,4-oxadiazol-2(3*H*)-one **14**

thermally to phenylcarbodiimide or phenylcyanamide, and these compounds cannot be formed directly from **14** or **15**, it is concluded that the formation of **5** and **8** takes place via benzonitrile imine **6** (Scheme 4). These experiments therefore lend support to the postulated formation of benzonitrile imine on FVT of tetrazole **2** (Scheme 3).

**Photolysis of 5-Phenyltetrazole 2.** 5-Phenyltetrazole **2** was photolyzed at 254 nm in Ar matrix at 12 K (Scheme 5). After 1

Scheme 5. Photolysis of 5-Phenyltetrazole **2**

min, new peaks were observed (Figure 1). Analysis of the rate of growth of the IR absorptions revealed that the bands at 2073, 1375, 1256, and 1072  $\text{cm}^{-1}$  belong to the same species. These values are in good agreement with anharmonic frequency calculations for C-phenylnitrile imine **6** [2140 (250), 1399 (20), 1275 (210), and 1104 (34)  $\text{cm}^{-1}$  (km/mol)] based on

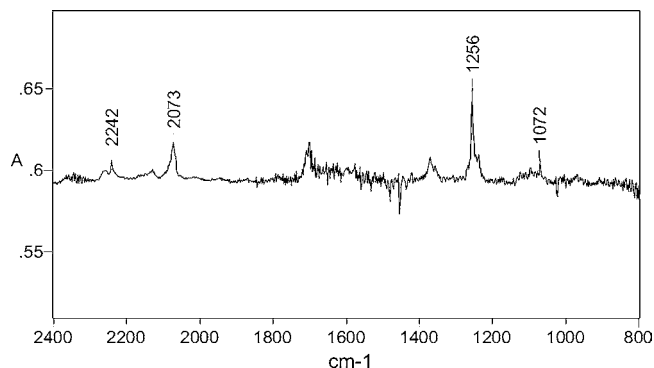


**Figure 1.** IR difference spectrum after 1 min photolysis (254 nm) of 5-phenyltetrazole **2** in Ar matrix at 12 K. Positive peaks: photolysis products, largely benzonitrile imine **6**; the peak near 1700  $\text{cm}^{-1}$  is due to an impurity on the deposition window. Negative peaks: reacted tetrazole **2**.

the B3LYP/6-31G\* structure. We usually use a scaling factor of 0.9613 for B3LYP/6-31G\* frequency calculations in the harmonic approximation.<sup>28</sup> The frequencies calculated in the anharmonic approximation are lower, and a scaling factor of 0.9676 for nitrile imines is more appropriate. This puts the calculated absorptions for **6** at 2071, 1354, 1234, and 1068  $\text{cm}^{-1}$ , in excellent agreement with experiment.

Figure 2 shows the changes in the IR spectrum in the range 2000–2400  $\text{cm}^{-1}$  as a function of photolysis times. A doublet at

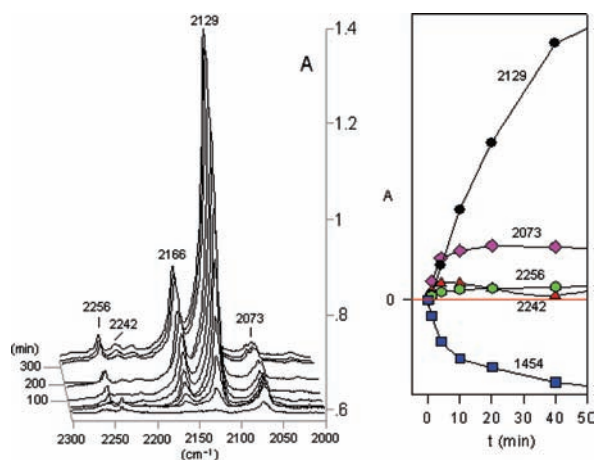


**Figure 2.** (Left) Partial IR difference spectra of 5-phenyltetrazole **2** at 12 K in Ar matrix at different photolysis times, showing peaks due to the photolysis products. Peaks at 2129 and 2166  $\text{cm}^{-1}$  are due to PhN=C=NH **5**. The peak at 2073  $\text{cm}^{-1}$  is assigned to PhC=NNH **6**. Ordinate in absorbance units. (Right) Plots of IR absorbances at different wavelengths versus photolysis time. Ordinate in relative absorbance units.

2129/2166  $\text{cm}^{-1}$  due to phenylcarbodiimide **5** formed immediately and kept increasing at longer photolysis times, whereas the peak at 2073  $\text{cm}^{-1}$  ascribed to nitrile imine **6** increased initially and then decreased. The small peak at 2242  $\text{cm}^{-1}$  also increased initially and then decreased. It is discussed further below. A weak peak at 2256  $\text{cm}^{-1}$  belongs to phenylcyanamide **8**. Both the signals at 2129 and 2167  $\text{cm}^{-1}$  belong to phenylcarbodiimide **5**. We have calculated the IR spectrum of phenylcarbodiimide **5** taking anharmonicity into account and find that a double band is indeed expected in the 2100  $\text{cm}^{-1}$  region. The unscaled NCN symmetrical stretching vibration  $\nu_{22}$  is calculated at 2210  $\text{cm}^{-1}$ , but a combination  $\nu_3 + \nu_{17}$  falls within 10  $\text{cm}^{-1}$ , at 2201  $\text{cm}^{-1}$ . Hence, these two absorptions can engage in Fermi resonance. Both modes  $\nu_3$  and  $\nu_{17}$  involve coupling between a ring deformation and the CN stretch. For this reason, arylcarbodiimides will often exhibit double bands, as observed,<sup>29</sup> but as this depends on ring deformations, it can be influenced by substitution. For example, we find that *N*-(3-pyridyl)carbodiimide exhibits only a single strong calculated NCN stretching band at 2211  $\text{cm}^{-1}$ .

The possibility that the 2073  $\text{cm}^{-1}$  band might belong to phenyldiazomethane **11** was ruled out by comparison of the IR spectra. **11** absorbs at 2066, 1601, 1500, and 1388  $\text{cm}^{-1}$  in Ar matrix, in agreement with a previously published spectrum<sup>30</sup> (Figure S2). It is known that an Ar matrix containing certain amounts of nitrogen can cause the IR frequencies to shift to higher values.<sup>31</sup> In the photolysis of tetrazole **2**, the eliminated nitrogen will remain in the Ar matrix and could cause such an IR frequency shift. By generating Ar matrices of **11** from **10**

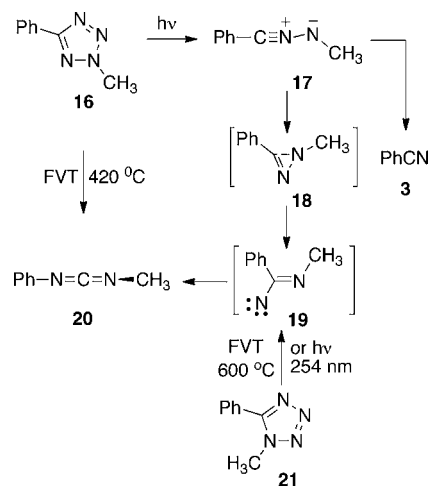
with addition of different amounts of nitrogen in the matrix, it was shown that the maximum shift is only about 4  $\text{cm}^{-1}$  (diazo stretch of **11** in Ar with 0% N<sub>2</sub>, 2066  $\text{cm}^{-1}$ ; with 17% N<sub>2</sub>, 2068  $\text{cm}^{-1}$ ; with 50% N<sub>2</sub>, 2069  $\text{cm}^{-1}$ ; and with 100% N<sub>2</sub>, 2070  $\text{cm}^{-1}$ ). Furthermore, phenyldiazomethane **11** disappears rapidly on photolysis in its UV maximum at 272 nm, whereas the 2073  $\text{cm}^{-1}$  absorption in the photoproducts of **2** remained unchanged. Therefore, the 2073  $\text{cm}^{-1}$  band in the Ar matrix of **2** cannot be due to diazo compound **11**.

The origin of the weak peak at 2242  $\text{cm}^{-1}$  (Figures 1 and 2) is unknown. The calculated structure of *C*-phenylnitrile imine **6**, corresponding to the 2073  $\text{cm}^{-1}$  absorption, is allenic (see the Calculations section). However, there is a second, propargylic minimum very close in energy (1–3 kcal/mol). As expected, the propargylic form absorbs at higher calculated frequency (anharmonic, scaled 2222  $\text{cm}^{-1}$ ). It is not very likely that the 2242  $\text{cm}^{-1}$  signal corresponds to the propargylic form of **6**, but the weakness of the signal makes an assignment impossible.

In summary, we can describe the photolysis reaction as follows. Photolysis of tetrazole **2b** causes elimination of N<sub>2</sub> and formation of benzonitrile imine **6** (2073  $\text{cm}^{-1}$ ) (Scheme 5). Under the photolysis conditions, **6** is short-lived and rearranges to carbodiimide **5** (2129/2166  $\text{cm}^{-1}$ ), probably via 1*H*-diazirine **7** or a similar intermediate. A second route to phenylcarbodiimide **5** is via the 1*H*-tautomer **2a** and the imidoylnitrine **4** (Scheme 5). The small amount of cyanamide **8** (2256  $\text{cm}^{-1}$ ) observed can be due to the tautomerization of **5**, which is hindered by the matrix environment. The photochemical rearrangement of the unsubstituted nitrile imine HCNNH **1** to cyanamide has been described.<sup>14,32</sup>

**C-Phenyl-*N*-methylnitrile Imine 17.** For the generation of *N*-methyl-*C*-phenylnitrile imine (*N*-methylbenzonitrile imine) **17**, tetrazole **16** was matrix-isolated in Ar and subjected to 254 nm photolysis, and the reaction was monitored by IR spectroscopy (Scheme 6 and Figures 3 and 4).

#### Scheme 6. Photolysis of 2-Methyl-5-phenyltetrazole **16**



During the first 3 min of photolysis, a complex peak at 2032/2016  $\text{cm}^{-1}$  was observed, together with a strong peak at 1361  $\text{cm}^{-1}$  (Figure 3), and  $\lambda_{\text{max}} = 285$  nm was recorded in the UV spectrum (Ar, 12 K). These absorptions are assigned to the nitrile imine **17** (Scheme 6) on the basis of the excellent agreement with the calculated anharmonic, scaled frequencies: 2038 (269) and 1341 (231)  $\text{cm}^{-1}$  (km/mol). The 2038  $\text{cm}^{-1}$

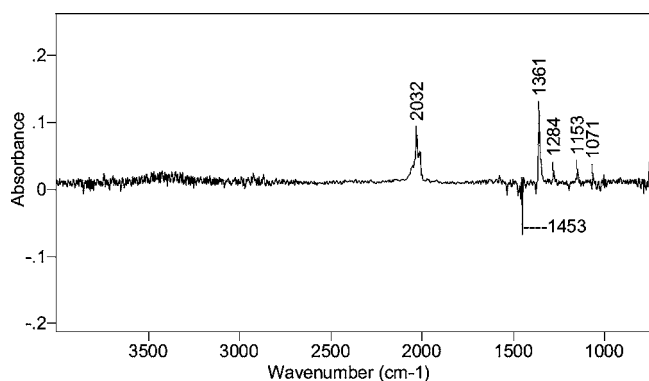


**Figure 3.** IR difference spectrum obtained after 254 nm photolysis of 2-methyl-5-phenyltetrazole **16** in Ar matrix at 12 K. Negative peaks: starting material. Positive peaks: product formed.

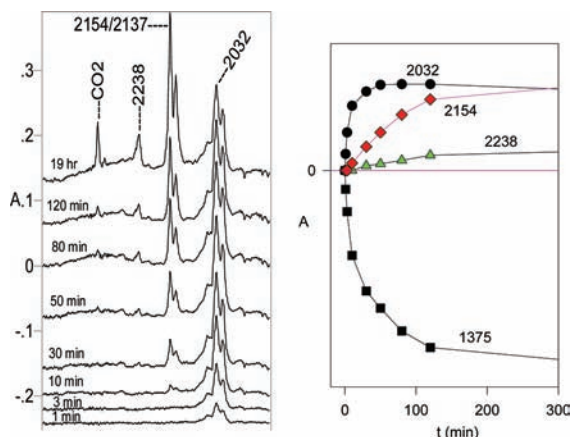


**Figure 4.** (Left) Partial IR difference spectra of tetrazole **16** at 12 K in Ar matrix at different photolysis times at 254 nm. The positive peaks are due to the photolysis products. The peaks at 2154 and 3137  $\text{cm}^{-1}$  belong to the same compound, *N*-methyl-*N'*-phenylcarbodiimide **20**. Abscissa 1900–2500  $\text{cm}^{-1}$ . (Right) Plots of IR absorbances at different wavenumbers versus photolysis time. The 1375  $\text{cm}^{-1}$  band belongs to the starting material **16**. Ordinates in arbitrary absorbance units.

band is due to the CNN asymmetric stretch. The 1341  $\text{cm}^{-1}$  band is due to the  $\text{CH}_3$  umbrella vibration. These are the only strong, calculated IR absorptions. The calculated vibration at 2038  $\text{cm}^{-1}$  is composed of 27%  $\nu_{31}$  ( $\nu_{\text{CNN}}$ ) and 16%  $\nu_2 + \nu_{26}$ . This may be the cause of the splitting observed in the experimental spectrum (2032, 2016  $\text{cm}^{-1}$ ).

During further photolysis from 3 to 120 min, new peaks at 2238 (assigned to benzonitrile **3**) and 2154/2137  $\text{cm}^{-1}$  (assigned to carbodiimide **20**) were increasing, while the 2032/2016  $\text{cm}^{-1}$  band decreased (Figure 3). These trends continued on further photolysis for up to 19 h. The last-appearing peaks at 2238 (benzonitrile **3**) and 2154/2137  $\text{cm}^{-1}$  (**20**) increased with different rates and hence belong to different compounds (Figure 3). The double peak at 2154/2137  $\text{cm}^{-1}$  (**20**) was increasing throughout the photolysis. Carbodiimide **20** is an unstable but isolable compound, which has been characterized on the basis of its IR (film), NMR, and mass spectra.<sup>17</sup> The rearrangement of **17** to **20** and **3** also took place on photolysis at 298 nm.

FVT of either 2-methyl-5-phenyltetrazole **16** (420 °C) or 1-methyl-2-phenyltetrazole **21** (430 °C) with Ar matrix isolation of the product at 12 K again produced *N*-methyl-*N'*-phenylcarbodiimide **20** (2154/2136  $\text{cm}^{-1}$ ). This compound

became the dominant product at 600 °C (Figure 5). Imidoylnitrene **19** is assumed to be an intermediate in both reactions (Scheme 6).

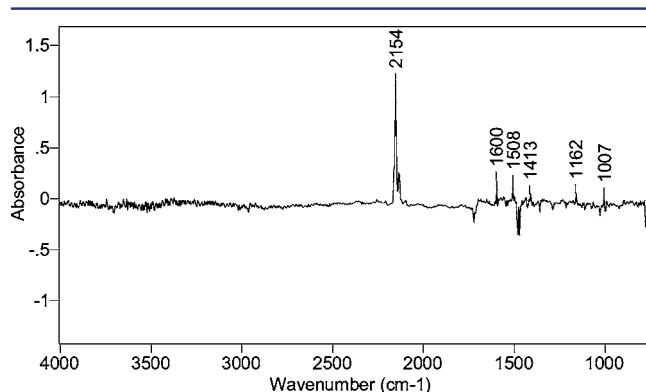


**Figure 5.** IR difference spectrum obtained from FVT (600 °C) of 1-methyl-5-phenyltetrazole **21** with Ar matrix isolation of the product at 12 K. Negative peaks: tetrazole **21** consumed in the reaction. The positive spectrum is assigned to the formed *N*-methyl-*N'*-phenylcarbodiimide **20**: 2154, 2136, 1600, 1508, 1413, and 1162  $\text{cm}^{-1}$ ; calcd anharmonic, scaled 2135 (1031), 2107 (23), 1565 (55), 1474 (23), 1429 (49), and 1111 (87)  $\text{cm}^{-1}$  (km/mol).

**C-Phenyl-*N*-trimethylsilylnitrile Imine (*N*-Trimethylsilylbenzonitrile Imine **23**).** Photolysis of the matrix-isolated 5-phenyl-2-trimethylsilyltetrazole **22** for 1 min at 254 nm resulted in the generation of new peaks at 2245, 1393, 1108, and 852  $\text{cm}^{-1}$  (Figure 6b), assigned to nitrile imine **23** (Scheme 7) due to the excellent agreement with the calculated spectrum (harmonic calculation at the B3LYP/6-31G\* level in Figure

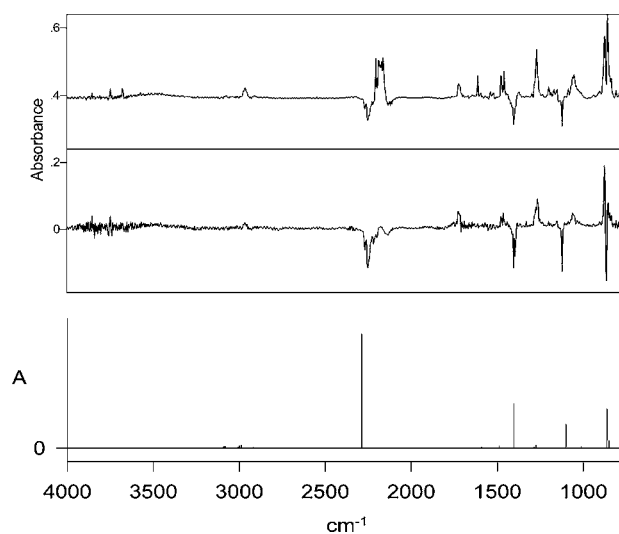
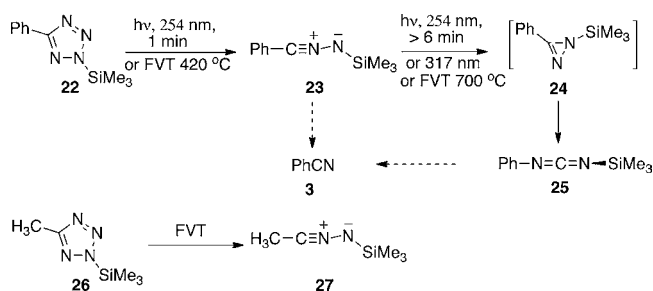


**Figure 6.** (a, bottom) Calculated IR spectrum of *C*-phenyl-*N*-(trimethylsilyl)nitrile imine **23** (B3-LYP/631G\*, harmonic wavenumbers scaled by 0.9613; ordinate in arbitrary absorbance units). (b, middle) *C*-Phenyl-*N*-(trimethylsilyl)nitrile imine **23** obtained by photolysis of tetrazole **22** at 254 nm for 1 min in Ar matrix at 12 K and then destroyed by photolysis at 314 nm for 7 min, giving rise to the difference spectrum. Negative peaks are due to the nitrile imine **23**: 2245, 1394, 1385, 1108, and 851  $\text{cm}^{-1}$ . Positive peaks are due to the formed *N*-phenyl-*N'*-(trimethylsilyl)carbodiimide **25**: 2140–2175, 1590, 1466, 1451, 1256, 1150, 862, and 848  $\text{cm}^{-1}$ . (c, top) IR difference spectrum after photolysis of **22** for 45 min in Ar matrix at 12 K.

## Scheme 7. C-Phenyl-N-trimethylsilylnitrile Imine



6a). The anharmonic, scaled wavenumbers are 2347 (1488), 1373 (597), 1085 (312), and 851 (478)  $\text{cm}^{-1}$  (km/mol), in excellent agreement with the experimental observation. The Ar matrix containing **23** shows a broad UV maximum at 325 nm. On further photolysis of the matrix at either 314 or 254 nm, the peaks due to **23** vanished from the IR spectrum, and a complex peak appeared at 2140–2175  $\text{cm}^{-1}$  (Figures 6 and 7). This is

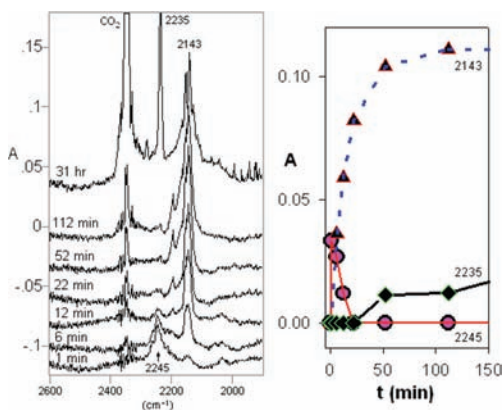


**Figure 7.** Partial IR difference spectra of 5-phenyl-2-(trimethylsilyl)tetrazole **22** at 12 K in Ar matrix at different photolysis times at 254 nm, showing peaks due to photolysis products. Abscissa 1900–2600  $\text{cm}^{-1}$ . (Right) Plots of IR absorbance of different wavenumbers versus photolysis time from 0 to 150 min. The 2245 and 2143  $\text{cm}^{-1}$  bands are assigned to nitrile imine **23** and carbodiimide **25**, respectively, and the 2235  $\text{cm}^{-1}$  band is assigned to benzonitrile.

assigned to *N*-phenyl-*N'*-(trimethylsilyl)carbodiimide **25**, which was also obtained by FVT of tetrazole **22** at 700 °C and identified by comparison with an authentic sample.<sup>33</sup> After 22 min of photolysis of the matrix at 254 nm, no 2245  $\text{cm}^{-1}$  band could be seen, but the 2143  $\text{cm}^{-1}$  band kept growing (Figure 7). After 52 min, a peak at 2235  $\text{cm}^{-1}$  started to grow and eventually became the strongest in the spectrum. After 31 h photolysis, the complex peak at 2143–2170  $\text{cm}^{-1}$  began to decrease (Figure 7). Nitrile imine **24** has also been generated by FVT of **22** at 420–430 °C and isolated at 77 K (IR neat: 2221, 1379, 1108, and 846  $\text{cm}^{-1}$  (Figure S5)).<sup>34</sup> The IR spectrum of an Ar matrix of the FVT product generated in this way was identical with the one obtained by photolysis.

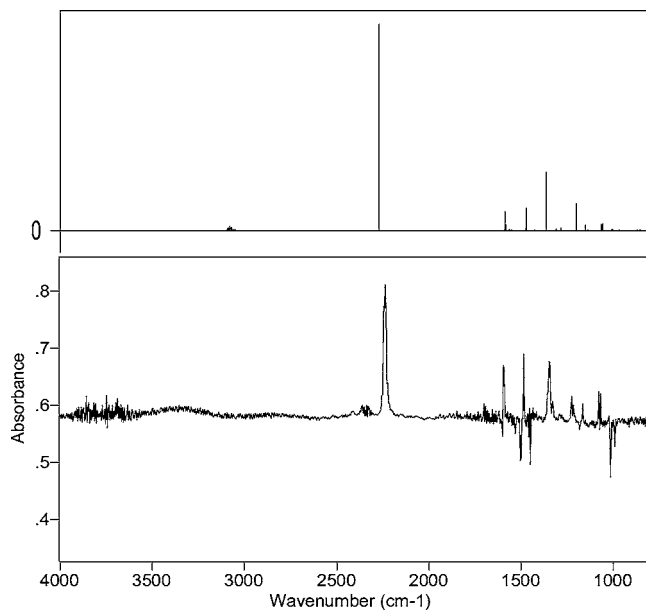
The initially weak peak at 2235  $\text{cm}^{-1}$  which grew on extended photolysis (Figure 7) is assigned to benzonitrile **3**. The 3  $\text{cm}^{-1}$  difference in the CN stretching vibrations in Figures 4 and 7 is presumably due to the different matrix environments. A mixture of carbodiimide **25** and benzonitrile is also formed on FVT of **22** at 700 °C.

Several other *N*-silylnitrile imines have been prepared by FVT of the corresponding 5-aryl- and 5-methyl-2-silyltetra-

zoles.<sup>34</sup> They all have strong IR absorptions at high wavenumbers, in the range 2230–2260  $\text{cm}^{-1}$ , indicating that they have propargylic structures. For example, the IR spectrum of *C*-methyl-*N*-trimethylsilylnitrile imine **23**, obtained by analogous photolysis of tetrazole **26** (Scheme 7), is in excellent agreement with the calculated spectrum at the B3LYP/6-31G\* level.<sup>35</sup>

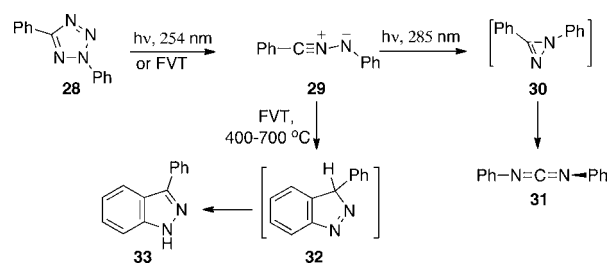
**Diphenylnitrile Imine (*N*-Phenylbenzonitrile Imine **29**).** *Photolysis of Diphenyltetrazole 28.* Toubro and Holm<sup>15</sup> carried out photolysis (250 nm) of 1,3-diphenyltetrazole **34** in a PVC film at 85 K and observed diphenylnitrile imine **29** by UV (377 nm) and IR (2228  $\text{cm}^{-1}$ ). The UV spectrum was also reported by Meier, Heinzelmann, and Heimgartner (ether/pentane/ethanol-glass, 77 K).<sup>36</sup> In order to compare with the other matrix results, we investigated the photolysis of tetrazole **28** in Ar matrix.

Tetrazole **28** was matrix-isolated in Ar at 12 K and subsequently subjected to photolysis at 254 nm. After 1 min, IR spectroscopic detection showed that the amount of **28** had diminished and a new compound had been formed. This compound had a very strong IR absorption at 2242  $\text{cm}^{-1}$ , together with other absorptions at 1598, 1490, 1349, 1228, 1169, 1079, and 1071  $\text{cm}^{-1}$ . During further photolysis for up to 93 min, the amount of this compound increased all the time. Figure 8 shows the IR difference spectrum after 3 min



**Figure 8.** (Top) Calculated IR spectrum of diphenylnitrile imine **29** [B3LYP/6-31G\*, anharmonic wavenumbers: 2306 (1066), 1610 (102), 1472 (140), 1348 (316), 1230 (176), 1184 (31), 1091 (32), and 1085 (46)  $\text{cm}^{-1}$  (km/mol)]. Ordinate in arbitrary absorbance units. (Bottom) Photolysis of 1,3-diphenyltetrazole **28** for 3 min in Ar matrix at 12 K; positive peaks are due to nitrile imine **29**: 2242, 1598, 1490, 1349, 1228, 1169, 1079, and 1071  $\text{cm}^{-1}$ .

photolysis. The new absorptions are assigned to diphenylnitrile imine **29** (Scheme 8), since the IR spectrum is in excellent agreement with the calculated spectrum at the B3LYP/6-31G\* level (Figure 8). Nitrile imine **29** features a broad UV absorption maximum at 385 nm, which tails into the visible spectrum up to ca. 420 nm in the Ar matrix (Figure S6). The intensity of this band decreased synchronously with the IR absorption of **29** on further photolysis.

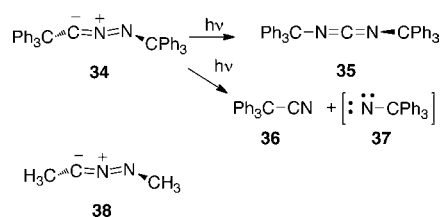
Scheme 8. *C,N*-Diphenylnitrile Imine

Further photolysis of diphenylnitrile imine **29** at 370 nm (monochromator) for 220 min caused the IR spectrum to disappear and new peaks to form at 2150/2141/2117  $\text{cm}^{-1}$ , which are assigned to diphenylcarbodiimide **31** (Figure S7) in agreement with the observations of Toubro and Holm.<sup>15</sup> The multiple splitting of the absorption is ascribed to Fermi resonance, as explained for *N*-phenylcarbodiimide **5** above. Additional peaks due to benzonitrile (2235  $\text{cm}^{-1}$ ) and 1-aza-1,2,4,6-cycloheptatetraene (1893  $\text{cm}^{-1}$ )<sup>37</sup> formed by cleavage of the nitrile imine<sup>15,37–39</sup> were also present (Figure S7).

FVT of diphenyltetrazole **28** causes cyclization of diphenylnitrile imine **29** to the 3*H*-3-phenylindazole **32**, followed by tautomerization to 3-phenylindazole **33** (Scheme 8).<sup>23</sup> The nitrile imine was not observable under these conditions (Figure S8).

**Bis(triphenylmethyl)nitrile Imine 34.** Bis-(triphenylmethyl)nitrile imine (*C,N*-ditritylnitrile imine **34**) is a stable compound, synthesized by reaction of bis-(trimethylstannyl)diazomethane with triphenylmethyl chloride in acetonitrile at  $-30\text{ }^{\circ}\text{C}$ .<sup>40</sup> As **34** is very nonvolatile, it cannot be sublimed without decomposition; hence, a full spectrum of matrix-isolated **34** in Ar was not obtainable, but the strong CNN stretching vibration was observed at 2049  $\text{cm}^{-1}$ .

Therefore, a KBr mull of **34** was produced, mounted on a cryostat window, and cooled to 12 K followed by broad-band photolysis. After 1 h of irradiation, the IR difference spectrum (Figure 9) showed the disappearance of nitrile imine **34** (2048, 2051  $\text{cm}^{-1}$ ) and formation of rearranged product, carbodiimide **35** (2125  $\text{cm}^{-1}$ ) (Scheme 9). On further irradiation for up to

Scheme 9. *C,N*-Ditritylnitrile Imine **34**

21 h, a new peak at 2236  $\text{cm}^{-1}$  appeared (Figure 9). Comparison with the authentic compound<sup>41</sup> also in KBr matrix at 12 K confirmed that this new peak was due to triphenylacetone nitrile **36**, presumably formed by cleavage of the nitrile imine to the nitrile and tritylnitrene **37** (not observed) (Scheme 9).

The X-ray crystal structure<sup>40</sup> of **34** demonstrates a distinctly allenic molecule. The allenic nature is further corroborated by the diastereoselective 1,3-dipolar cycloaddition of **34** in solution.<sup>4</sup> The calculated structure of the model compound  $\text{H}_3\text{C-CNN-CH}_3$  **38** (Table 1) is in fairly good agreement with the experimental structure of **34**. The anharmonic calculation of the vibrational spectrum of **38** also indicates an allenic molecule (CNN sym. stretch, scaled, 2056  $\text{cm}^{-1}$  (411  $\text{km/mol}$ )), in good agreement with the experimental value for **34**.

**Bis[bis(diisopropylamino)boryl]nitrile Imine 39.** Bis-[bis(diisopropylamino)boryl]nitrile imine **39**, synthesized from the reaction of the lithium salt of [bis(diisopropylamino)boryl]diazomethane with the corresponding chloroborane at room temperature, is a stable and distillable compound.<sup>42</sup> This nitrile imine was matrix-isolated in Ar at 12 K by sublimation at  $75\text{ }^{\circ}\text{C}$  ( $10^{-5}$  mbar) with Ar as a carrier gas. The IR spectrum shows a very strong CNN absorption at 2177  $\text{cm}^{-1}$  (Figure 10).

Irradiation of this matrix using broadband UV light (1000 W high-pressure Xe/Hg lamp) caused conversion of **39** to carbodiimide **40** (Scheme 10). The first 23 min of the reaction followed first-order kinetics ( $t_{1/2} = 7.6$  min). After 23 min, the rate of reaction slowed, as is often observed in matrices.<sup>43</sup> The IR difference spectrum after 43 min of irradiation demonstrated a clean rearrangement of **39** (Figure 10). In the UV spectrum, **39** has a broad band at 290 nm, which also disappeared completely after 43 min of irradiation. Bertrand et al. observed that the photo-rearrangement of nitrile imine **39** to carbodiimide **40** also takes place in benzene solution.<sup>42</sup>

The frequency of the nitrile imine CNN stretch is relatively low in this case (2177  $\text{cm}^{-1}$ ), and that for the carbodiimide NCN stretch is extraordinarily high (2245  $\text{cm}^{-1}$ ). The X-ray structure of the analogous bis[bis(dicyclohexylamino)boryl]nitrile imine **41** demonstrates a distinctly propargylic structure with a nearly linear B-C-N-N moiety.<sup>13g</sup> This structure is understandable in terms of a favorable overlap between an empty p orbital on boron with the CN triple bond. The short B–N bond (1.45 Å) indicates delocalization of the negative charge on the terminal N onto boron. The calculated structure of the model compound  $\text{H}_2\text{B-CNN-BH}_2$  **42** (Table 1) is in good agreement with the experimental X-ray structure of **41**. The calculated anharmonic, scaled CNN stretching vibration for **42** is 2173  $\text{cm}^{-1}$  (Table 2), in very good agreement with the experimental value for **41**, 2177  $\text{cm}^{-1}$ .

## ■ CALCULATIONS

The structures of nitrile imines were investigated by density functional theory at the B3LYP/6-31G\* level using the

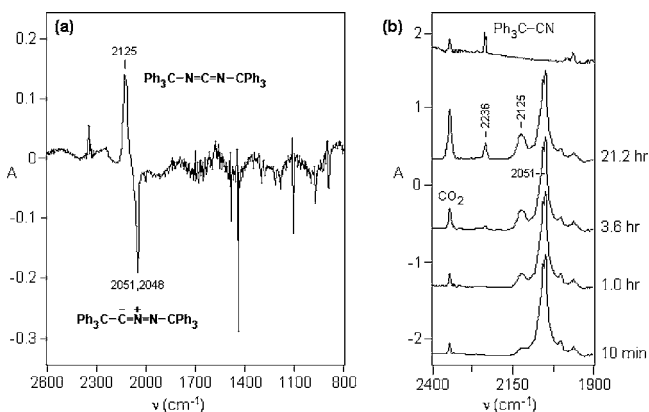


**Figure 9.** (a) IR difference spectrum obtained after 1 h of irradiation of bis(trityl)nitrile imine **34** in KBr matrix at 12 K. The positive peaks are due to the formed bis(trityl)carbodiimide **35** (2125  $\text{cm}^{-1}$ ). Negative peaks are due to reacted nitrile imine **34** (2048, 2051  $\text{cm}^{-1}$ ). (b) Partial IR spectra obtained from irradiation of **34** at 12 K in KBr matrix at different times. The top spectrum is that of the authentic triphenylmethyl cyanide **36** (2236  $\text{cm}^{-1}$ ) in KBr matrix at 12 K.

Table 1. Calculated (B3LYP/6-31 G\*) Structural Data for Nitrile Imines (R-CNN-R') and the Transition States for Inversion<sup>a,b</sup>

R,R' structure <sup>a</sup>	r(R-C)	r(C-N)	r(N-N)	r(N-R')	∠RCN	∠CNN	∠NNR'	τRCNN	τCNNR'
H,H 1A	1.080	1.199	1.245	1.028	129.2	169.1	109.0	221.7	227.7
1P <sup>b</sup>	1.063	1.171	1.258	1.024	179.9	172.1	108.9	185.6	180.1
C <sub>6</sub> H <sub>5</sub> ,H 6A	1.445	1.195	1.253	1.028	141.6	169.2	108.9	232.8	218.7
C <sub>6</sub> H <sub>5</sub> ,H 6P	1.418	1.175	1.265	1.025	179.6	171.5	100.4	72.6	179.4
H,C <sub>6</sub> H <sub>5</sub> 43A	1.082	1.200	1.242	1.417	128.9	169.4	117.3	213.0	137.8
H,C <sub>6</sub> H <sub>5</sub> 43P <sup>b</sup>	1.064	1.170	1.255	1.410	178.0	173.6	117.3	359.0	180.1
C <sub>6</sub> H <sub>5</sub> ,CH <sub>3</sub> 17A	1.416	1.177	1.257	1.467	177.7	174.2	113.4	11.1	179.1
C <sub>6</sub> H <sub>5</sub> , Si(CH <sub>3</sub> ) <sub>3</sub> 23P	1.420	1.176	1.250	1.763	177.9	175.2	123.2	357.6	181.1
23P <sup>b</sup>	1.420	1.167	1.248	1.762	178.5	178.1	132.9	347.7	243.5
C <sub>6</sub> H <sub>5</sub> ,C <sub>6</sub> H <sub>5</sub> 29P	1.416	1.174	1.263	1.405	178.2	172.6	117.1	1.3	179.9
29A <sup>b</sup>	1.431	1.220	1.235	1.412	144.7	169.6	116.8	233.0	221.3
CH <sub>3</sub> ,CH <sub>3</sub> 38A	1.483	1.196	1.247	1.471	138.1	170.3	113.3	215.0	236.5
38P <sup>b</sup>	1.495	1.174	1.254	1.469	175.5	174.9	113.9	309.1	188.8
BH <sub>2</sub> ,BH <sub>2</sub> 42P	1.486	1.184	1.230	1.397	177.1	172.2	137.8	180.0	180.0
42P <sup>b</sup>	1.494	1.179	1.254	1.438	178.8	173.2	118.5	204.5	188.7

<sup>a</sup>Bond lengths in angstroms and angles in degrees. Major canonical structures denoted by A for allenic and P for propargylic. <sup>b</sup>Transition state.

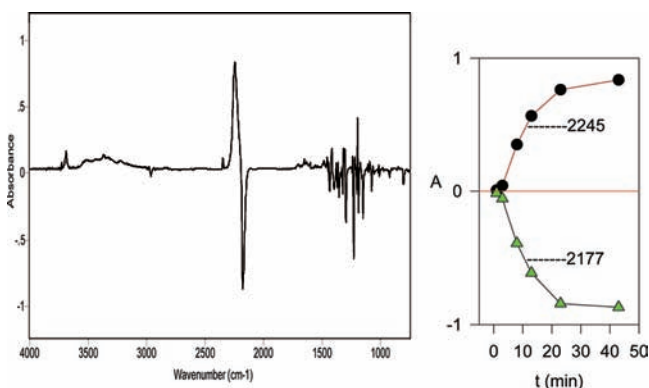


**Figure 10.** (Left) IR difference spectrum obtained after irradiation of bis(boryl)nitrile imine **39** at 12 K in Ar matrix for 43 min. Abscissa 750–4000 cm<sup>-1</sup>. The positive peaks (2245 cm<sup>-1</sup>) are due to the formation of bis(boryl)carbodiimide **40**; the negative peaks (2177 cm<sup>-1</sup>) are due to reacted nitrile imine **39**. (Right) Relative absorbances of nitrile imine **39** and carbodiimide **40** at 12 K in Ar matrix after different irradiation times (0–40 min) with broadband UV light (high-pressure Xe/Hg lamp).

Gaussian 09 suite of programs.<sup>44</sup> Table 1 lists the calculated structural data, which permit classification of the nitrile imines as either allenic (A) or propargylic (P). This geometrical classification is supported by NBO calculations at the

#### Scheme 10. Bis[bis(diisopropylamino)boryl]nitrile Imine **39**

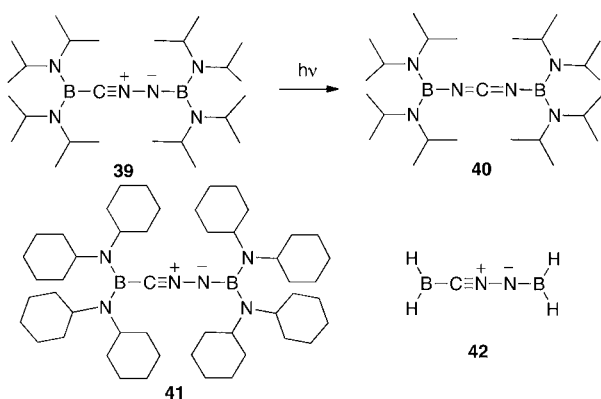


**Table 2. Harmonic and Anharmonic Calculated and Experimental IR Wavenumbers (cm<sup>-1</sup>) of the CNN Moiety in Nitrile Imines RCNNR' and Their Transition States for Inversion**

substituents, R,R' structure <sup>a</sup>	IR		
	calcd <sup>b</sup> harmonic	calcd <sup>b</sup> anharmonic	exptl
H,H 1A	2065	2033	2033 (Ar) <sup>c</sup>
H,H 1P <sup>d</sup>	2189	2118	
C <sub>6</sub> H <sub>5</sub> ,H 6A	2123	2071	2073 (Ar)
C <sub>6</sub> H <sub>5</sub> ,H 6P	2288	2222	
H,C <sub>6</sub> H <sub>5</sub> 43A	2043	2009	2014 (PVC) <sup>e</sup>
H,C <sub>6</sub> H <sub>5</sub> 43P <sup>d</sup>	2173	2132	
C <sub>6</sub> H <sub>5</sub> ,CH <sub>3</sub> 17A	2087	2038	2032 (Ar)
C <sub>6</sub> H <sub>5</sub> ,CH <sub>3</sub> 17P <sup>d</sup>	2274	2203	
C <sub>6</sub> H <sub>5</sub> ,Si(CH <sub>3</sub> ) <sub>3</sub> 23P	2288	2247	2245 (Ar)
23P <sup>d</sup>	2339	2289	
C <sub>6</sub> H <sub>5</sub> ,C <sub>6</sub> H <sub>5</sub> 29P	2273	2226	2242 (Ar)
CH <sub>3</sub> ,CH <sub>3</sub> 38A	2107	2062	(2050) <sup>f</sup>
38P <sup>d</sup>	2305	2285	
BH <sub>2</sub> ,BH <sub>2</sub> 42P	2213	2173	(2177) <sup>g</sup>
42P <sup>d</sup>	2201	2162	

<sup>a</sup>The major canonical structures are denoted by A for allenic and P for propargylic. <sup>b</sup>Scaling factor 0.9613 (ref 28) for calculated harmonic wavenumbers and 0.9676 for the corresponding anharmonic calculations (see text). <sup>c</sup>Ref 14. <sup>d</sup>Transition state. <sup>e</sup>Ref 15. <sup>f</sup>Experimental value for the ditryl compound **38**. <sup>g</sup>Experimental value for the bis(diisopropyl)amino compound **39**.

CCSD(T) level, which reveal the corresponding allenic and propargylic electronic structures (see Supporting Information). NBO calculations will be discussed more thoroughly in a forthcoming publication. Vibrational frequencies in the harmonic approximation were calculated at the B3LYP/6-31G\* level. The vibrational Schrödinger equation was solved by a perturbation–variation procedure taking into account the rotational contribution to anharmonicity by employing the P\_MWCI2 methodology and parallelization described previously.<sup>45–47</sup> Key data are listed in Table 2, and a complete listing with spectroscopic descriptions is given in the Supporting Information. A scaling factor of 0.9613 is commonly used for harmonic calculations of wavenumbers at the B3LYP/6-31G\* level.<sup>28</sup> A scaling factor has also been used



to determine the wavenumbers in the double hypothesis of electrical and mechanical anharmonicities, as it is not currently possible to construct variationally and diagonalize the complete vibrational Hamiltonian for molecules of the sizes and complexities considered here (e.g.,  $N_{\text{vib}}[\text{PhCnNSi}(\text{Me})_3] = 45$ ). Thus, we have used a slightly different scaling factor of 0.9676 for all the anharmonic wavenumbers of nitrile imines at the B3LYP/6-31G\* level in the present work. Potential energy surface calculations at X/B3LYP//Y/6-31G\* levels (X = QCISD or CCSD(T), Y = cc-pVTZ or 6-31G\*) were performed for reference systems by using procedures reported elsewhere.<sup>48</sup>

In general, planar, propargylic, nitrile-like structures with short C≡N triple bonds and N—N single bonds correspond to high IR frequencies in the 2200–2300  $\text{cm}^{-1}$  range. A longer CN bond and a shorter NN bond correspond to a more nonplanar, allenic structure with a lower IR frequency in the range 2000–2100  $\text{cm}^{-1}$ .

The calculated data in Table 2 show mostly very good agreement with the available experimental data. High-level calculations predict an allenic form for HCNNH **1**.<sup>3,14,49</sup> Our calculations at the B3LYP/6-31G\*, G4MP2, G3MP2B3, CBS-QB3, W1BD, and CCSD(T) levels confirm that the allenic form lies 2.5–4.1 kcal/mol below the propargylic form, and the latter is a TS for inversion of the allenic form (Tables 1–3 and

**Table 3. Calculated Energies of Selected Nitrile Imines RCNNR' at Various Levels of Theory**

substituents R,R' structure <sup>a</sup>	energies <sup>d</sup> (Hartree)	energy difference $E(\text{P}) - E(\text{A})$		
		B3LYP/6-31G* (kcal/mol)	CBS-QB3 (kcal/mol)	QCISD/6-31G* (kcal/mol)
H,H 1A	-148.6975867			<sup>e</sup>
H,H 1P <sup>b</sup>	-148.6911501	4.14	2.50	4.58
C <sub>6</sub> H <sub>5</sub> ,H 6A	-379.7631573			
C <sub>6</sub> H <sub>5</sub> ,H 6P <sup>c</sup>	-379.7622241	0.59	1.06	2.56
H,C <sub>6</sub> H <sub>5</sub> 43A	-379.7569613			
H,C <sub>6</sub> H <sub>5</sub> 43P <sup>b</sup>	-379.7506782	3.95	2.94	5.87
C <sub>6</sub> H <sub>5</sub> ,CH <sub>3</sub> 17A	-419.0751562			
C <sub>6</sub> H <sub>5</sub> ,CH <sub>3</sub> 17P <sup>b</sup>	-419.0737332	0.89	1.33	3.28
C <sub>6</sub> H <sub>5</sub> ,Si(CH <sub>3</sub> ) <sub>3</sub> 23P	-788.4706475			
23P <sup>b</sup>	-788.4698297	-0.51	-0.21	
CH <sub>3</sub> ,CH <sub>3</sub> 38A	-227.3333067			
38P <sup>b</sup>	-227.3276474	3.55	3.32	
BH <sub>2</sub> ,BH <sub>2</sub> 42P	-199.6489284			
42P <sup>b</sup>	-199.6473351	-1.00	-0.95	

<sup>a</sup>Major canonical structures denoted by A for allenic and P for propargylic. <sup>b</sup>Transition state for inversion. <sup>c</sup>6P is calculated to be a second minimum, not a TS. <sup>d</sup>B3LYP/6-31G\* energies. <sup>e</sup>Further energy differences between allenic and propargylic (TS) forms for HCNNH **1**: W1BD, 2.42; G3MP2B3, 3.01; and G4MP2, 3.12 kcal/mol.

Figure 11). The calculated, scaled, anharmonic CNN stretching vibrations at the B3LYP level are at 2033 (allenic) and 2118  $\text{cm}^{-1}$  (propargylic). The experimental wavenumber in Ar matrix is 2033  $\text{cm}^{-1}$ ,<sup>14</sup> thus confirming that the allenic form is observed. The anharmonicity calculation indicates that the cumulenic absorption band is composed of the CNN stretch (64%) together with  $\nu_3 + \nu_5$  (25%) (see Supporting Information). The validity of the B3LYP/6-31G\* calculations of IR spectra was checked by performing higher level

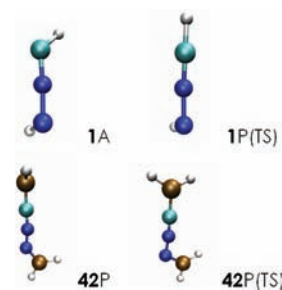


**Figure 11.** Ground states of an allenic (1A) and a propargylic (42P) nitrile imine and the transition states for their CH inversion (1P(TS)) or BH<sub>2</sub> rotation (42P(TS)) at the B3LYP/6-31G\* level.

vibrational calculations for HCNNH **1** and PhCnNH **6**, namely at the CCSD(T)/6-31G\* and CCSD(T)//B3LYP/cc-pVTZ/6-31G\* levels (Tables 4 and 5). It is seen that all the vibrational calculations are in agreement, and the anharmonic wavenumbers approach the experimental ones more closely at the higher level of theory.

The two monophenyl compounds, PhCnNH **6** and HCNNPh **43**, are predicted to have allenic structures similar to that of HCNNH **1** (Tables 1 and 2). Two minima very close in energy are calculated for **6**, one allenic **6A** and the other propargylic **6P** (Table 1). The allenic form **6A** is calculated to be only 0.6–2.6 kcal/mol below **6P** (Table 3). The interconversion of the two forms is illustrated in Figure 12. The calculated anharmonic, scaled frequencies are 2071 and 2222  $\text{cm}^{-1}$ , respectively (Table 2). The former is in excellent agreement with the observed absorption at 2073  $\text{cm}^{-1}$ .

In the case of HCNNPh **43**, the energy difference is 3–4 kcal/mol in favor of the allenic form **43A**. This energy ordering was confirmed at the CBS-QB3 level. The propargylic structure **43P** is a TS for the inversion of the allenic form. The calculated anharmonic, scaled frequencies are 2009 (**43A**) and 2132  $\text{cm}^{-1}$  (**43P**). Thus, only the allenic structure is in agreement with experiment (2014  $\text{cm}^{-1}$  in PVC film,<sup>15</sup> Table 2).

In PhCnNMe **17**, two minima were found with a CBS energy difference of 1.3 kcal/mol. The higher-lying minimum corresponds to a propargylic structure (anharmonic, scaled CNN stretch 2203  $\text{cm}^{-1}$ ). The lower minimum is allenic [anharmonic, scaled CNN stretch 2038  $\text{cm}^{-1}$  (269 km/mol)], in good agreement with the experimentally observed spectrum (2032  $\text{cm}^{-1}$ ; see Figure 4). A QCISD/6-31G\* calculation predicts the anharmonic allenic CNN stretch at 2073  $\text{cm}^{-1}$  (unscaled), very close to the experimental value, thereby suggesting a scaling factor close to unity (0.98) at this computational level.

Good agreement between calculated and observed IR spectra of PhCnNSiMe<sub>3</sub> **23** and PhCnNPh **29** was described above (Figures 6–8). These are typical planar, propargylic compounds with nearly linear Ph-CNN moieties and high CN stretching frequencies. The anharmonicity calculations indicate that the strong band for **23** observed at 2245  $\text{cm}^{-1}$  is due largely (92%) to the CNN symmetrical stretch (see Supporting Information for details). In H<sub>3</sub>C-CNN-Si(CH<sub>3</sub>)<sub>3</sub> **27**, too, the propargylic structure is predicted in agreement with the observed CN vibration at 2259  $\text{cm}^{-1}$ ,<sup>35</sup> although CH<sub>3</sub> monosubstitution on either C or N favors allenic structures. This stabilization of the propargylic forms by *N*-silyl substituents is in accord with the general observation that silicon stabilizes negative charges in the  $\alpha$ -position but positive charges in the  $\beta$ -position.

**Table 4. Harmonic ( $\omega$ ) and Anharmonic ( $\nu$ ) Calculated Wavenumbers ( $\text{cm}^{-1}$ ) for the Allenic Form of HCNNH 1 at Various Levels of Theory<sup>a</sup>**

B3LYP/6-31G*		QCISD/6-31G*		CCSD(T)/6-31G*		QCISD/cc-pVTZ		CCSD(T)/cc-pVTZ //6-31G*/6-31G*	
$\omega$	$\nu$	$\omega$	$\nu$	$\omega$	$\nu$	$\omega$	$\nu$	$\omega$	$\nu$
2147.5	2100.7	2088.2	2069.2	2091.0	2067.6	2084.1	2064.6	2080.5	2062.3

<sup>a</sup>Experimental wavenumber for HCNNH 1 is  $2033 \text{ cm}^{-1}$ .<sup>14</sup> The calculated wavenumbers are unscaled here to facilitate comparison of different computational methods. The complete calculated spectroscopic data is listed in the Supporting Information.

**Table 5. Harmonic ( $\omega$ ) and Anharmonic ( $\nu$ ) Calculated Wavenumbers ( $\text{cm}^{-1}$ ) for Allenic (A) and Propargylic (P) forms of PhCNNH 6 at Various Levels of Theory<sup>a</sup>**

QCISD/B3LYP//6-31G*/6-31G*			B3LYP/6-31G*		
$\omega$	$I$ (km/mol)	$\nu$	$\omega$	$I$ (km/mol)	$\nu$
6A					
2129.0	215	2089.4	2208.1	250	2139.6
6P					
2380.4	548	2295.8	2380.2	580	2296.2

<sup>a</sup>Experimental wavenumber for PhCNNH 6 is  $2073 \text{ cm}^{-1}$ . The calculated wavenumbers are unscaled here to facilitate comparison of different computational methods. The complete calculated spectroscopic data are listed in the Supporting Information.

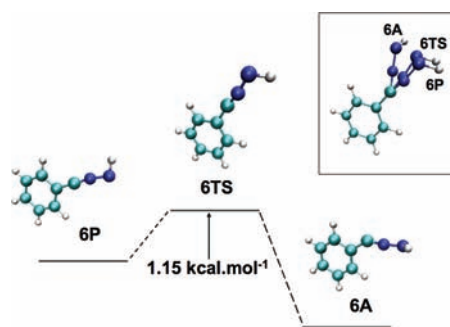


**Figure 12.** Schematic energy profile showing 6A, 6P, and the transition state connecting them at the B3LYP/6-31G\* level. Energy difference between 6P and 6A is  $0.59 \text{ kcal/mol}$  at this level (cf. Table 3). Inset: superposition of the three structures.

For  $\text{CH}_3\text{CNNCH}_3$  38, the anharmonicity calculations indicate that the strong ( $396 \text{ km/mol}$ ) allenic-type absorption at  $2062 \text{ cm}^{-1}$  (scaled; Table 2) is mostly due to the CNN symmetrical stretch (66%), which is coupled with  $\nu_2 + \nu_6$  and  $2\nu_3$  (see Supporting Information). The data further indicate that a methyl group is not a bad model for the trityl group,  $\text{Ph}_3\text{C}$  in these compounds: the calculated structure of  $\text{CH}_3\text{CNNCH}_3$  38 is not far from that of  $\text{Ph}_3\text{C-CNN-CPh}_3$  34, and both have IR absorptions in the allenic region (ca.  $2050 \text{ cm}^{-1}$ ; see above and Tables 1 and 2).

The propargylic structures of the bis-boryl compounds 39 and 41 are in good agreement with that calculated for the model compound  $\text{BH}_2\text{CNNBH}_2$  42 (Table 1). The CN stretching frequencies of 39 (experimental) and 42 (anharmonic calculation, scaled by 0.9676) are  $2177$  and  $2173 \text{ cm}^{-1}$ , respectively (Table 2). Delocalization of electron density from the CN triple bond to the vacant p orbital on boron stabilizes a nearly linear, propargylic structure. This structure can undergo  $\text{BH}_2$  rotation via a propargylic TS (Figure 11).

In contrast to the allenic and propargylic nitrile imines described above, nitrile imines carrying highly electronegative but lone-pair-donating substituents such as  $\text{NH}_2$ , OH, and F have been reported to possess a high degree of carbenic

character.<sup>5</sup> In agreement with this, our calculations of anharmonic vibrational spectra indicate that these compounds have very low and very weak frequencies in the  $1900\text{--}2000 \text{ cm}^{-1}$  range, and they can hardly be described as cumulenes. Moreover, NBO calculations at the CCSD(T) level are in agreement with partial carbenic/dipolar structures in these cases. These compounds will be the subjects of a separate publication.

## CONCLUSIONS

The nitrile imines Ph-CNN-H 6, Ph-CNN- $\text{CH}_3$  17, and Ph-CNN-Ph 29 were generated by Ar matrix photolysis of the corresponding tetrazoles. Ph-CNN- $\text{SiMe}_3$  23 was generated both photochemically and by FVT with matrix isolation.  $\text{Ph}_3\text{C-CNN-CPh}_3$  34 and  $((i\text{Pr})_2\text{N})_2\text{B-CNN-B}((i\text{Pr})_2\text{N})_2$  39 are stable compounds that were isolated and photolyzed in matrices.

The IR absorptions of nitrile imines were investigated by detailed calculations of the anharmonic vibrational spectra. In general, the results confirm that nitrile imines fall in two principal categories. Those with IR absorptions above  $2200 \text{ cm}^{-1}$  have essentially propargylic structures characterized by CN triple bonds (e.g., PhCNSiMe<sub>3</sub> 23, PhCNNPh 29, and  $\text{R}_2\text{B-CNN-BR}_2$  39 and 42). Nitrile imines with IR absorptions below ca.  $2100 \text{ cm}^{-1}$  have more allenic-type structures (e.g., HCNNH 1, PhCNNH 6, HCNNPh 43, PhCNNCH<sub>3</sub> 17, and  $\text{Ph}_3\text{C-CNN-CPh}_3$  34). Thus, the IR spectra of nitrile imines are found to reflect their structures accurately.

All the nitrile imines investigated here isomerize to the corresponding carbodiimides both thermally and photochemically. Monosubstituted NH-carbodiimides such as Ph-N=C=N-H 5 isomerize thermally to the corresponding cyanamides (e.g., PhNHCN 8), but this tautomerization is reversible under FVT conditions.

## EXPERIMENTAL SECTION

The apparatus for flash vacuum thermolysis (FVT), matrix isolation, and matrix photolysis was as previously described.<sup>50</sup> FVT was carried out in unpacked quartz tubes (100 mm length, 8 mm i.d.) at  $200\text{--}1000 \text{ }^\circ\text{C}$ , with or without Ar as a carrier gas (ca.  $10^{-4}$  mbar), and the products were isolated in Ar matrices on a KBr observation disk at  $12\text{--}20 \text{ K}$ , or neat at  $12$  or  $77 \text{ K}$ . When a KBr mull was used (compound 34), this was clamped to the KBr observation disk. The temperature was measured in the KBr disk. Photolyses were carried out with a low-pressure Hg lamp (75 W; 254 nm) or a high-pressure Xe-Hg lamp (1000 W) equipped with a monochromator. Infrared spectra were recorded at a resolution of  $1\text{--}0.5 \text{ cm}^{-1}$ . Melting points are uncorrected.

## ASSOCIATED CONTENT

### Supporting Information

Further Ar matrix IR spectra, experimental data, Cartesian coordinates and energies of calculated ground states and transition states, full details of anharmonic calculated wavenumbers and spectroscopic descriptions, and complete ref 44.

This material is available free of charge via the Internet at <http://pubs.acs.org>.

## AUTHOR INFORMATION

### Corresponding Author

wentrup@uq.edu.au

### Notes

The authors declare no competing financial interest.

## ACKNOWLEDGMENTS

This work was supported by the Australian Research Council. We are indebted to Prof. Guy Bertrand (Toulouse and Riverside) and Dr. David Kvaskoff (Queensland) for many stimulating discussions on nitrile imines and computational chemistry, respectively.

## REFERENCES

- (1) (a) Sharp, J. T. Nitrile ylides and nitrile imines. In *Synthetic Applications of 1,3-Dipolar Cycloaddition Chemistry Toward Heterocycles and Natural Products*; The Chemistry of Heterocyclic Compounds 59; Padwa, A., Pearson, W. H., Eds.; John Wiley & Sons: New York, 2002. (b) Kobayashi, S.; Jørgensen, K. A., *Cycloaddition Reactions in Organic Synthesis*; Wiley-VCH: Weinheim, 2002.
- (2) Caramella, P.; Houk, K. N. *J. Am. Chem. Soc.* **1976**, *98*, 6397.
- (3) Wong, M. W.; Wentrup, C. *J. Am. Chem. Soc.* **1993**, *115*, 7743.
- (4) Fauré, J.-L.; Réau, R.; Wong, M. W.; Koch, R.; Wentrup, C.; Bertrand, G. *J. Am. Chem. Soc.* **1997**, *119*, 2819–2824.
- (5) Mawhinney, R. C.; Muchall, H. M.; Peslherbe, G. H. *Chem. Commun.* **2004**, 1862–1063.
- (6) Mawhinney, R. C.; Peslherbe, G. H.; Muchall, H. M. *J. Phys. Chem. B* **2008**, *112*, 650–655.
- (7) Mawhinney, R. C.; Muchall, H. M.; Peslherbe, G. H. *Can. J. Chem.* **2005**, *83*, 1615–25.
- (8) Cargnoni, F.; Molteni, G.; Cooper, D. L.; Raimondi, M.; Ponti, A. *Chem. Commun.* **2006**, 1030.
- (9) Ess, D. H.; Houk, K. N. *J. Am. Chem. Soc.* **2008**, *130*, 10187.
- (10) Braid, B.; Waiter, C.; Engels, B.; Hiberty, P. C. *J. Am. Chem. Soc.* **2010**, *132*, 7631–7637.
- (11) Zheng, S.-L.; Wang, Y. W.; Coppens, P. *J. Am. Chem. Soc.* **2009**, *131*, 18036–18037.
- (12) Review of stable and unstable nitrile imines: Bertrand, G.; Wentrup, C. *Angew. Chem., Int. Ed. Engl.* **1994**, *33*, 527.
- (13) For stable nitrile imines bearing heteroatom substituents (B, Si, P) at both carbon and nitrogen: (a) Arthur, M. P.; Baceiredo, A.; Bertrand, G. *J. Am. Chem. Soc.* **1991**, *113*, 5062. (b) Castan, F.; Baceiredo, A.; Bertrand, G. *Angew. Chem., Int. Ed. Engl.* **1989**, *28*, 1250. (c) Castan, A.; Baceiredo, A.; Bigg, G.; Bertrand, G. *J. Org. Chem.* **1991**, *56*, 1801. (d) Granier, M.; Baceiredo, A.; Dartiguenave, Y.; Dartiguenave, M.; Menu, M. J.; Bertrand, G. *J. Am. Chem. Soc.* **1990**, *112*, 6277. (e) Granier, M.; Baceiredo, A.; Bertrand, G.; Huch, V.; Veith, M. *Inorg. Chem.* **1991**, *30*, 1161. (f) Reau, R.; Veneziani, G.; Bertrand, G. *J. Am. Chem. Soc.* **1992**, *114*, 6059. (g) Arthur, M. P.; Baceiredo, A.; Fischer, J.; De Cian, A.; Bertrand, G. *Synthesis* **1992**, 43.
- (14) Maier, G.; Eckwert, J.; Bothur, A.; Reisenauer, H. P.; Schmidt, C. *Liebigs Ann.* **1996**, 1041.
- (15) Toubro, N. H.; Holm, A. *J. Am. Chem. Soc.* **1980**, *102*, 2093.
- (16) Granier, M.; Baceiredo, A.; Bertrand, G. *Angew. Chem., Int. Ed. Engl.* **1988**, *27*, 1350–1351. Castan, F.; Baceiredo, A.; Bidd, D.; Bertrand, G. *J. Org. Chem.* **1991**, *56*, 1801.
- (17) Fischer, S.; Wentrup, C. *J. Chem. Soc., Chem. Commun.* **1980**, 502–503.
- (18) Granier, M.; Baceiredo, A.; Grutzmacher, H.; Pritzkow, H.; Bertrand, G. *Angew. Chem., Int. Ed. Engl.* **1990**, *29*, 659–661.
- (19) For evidence for a 1*H*-diazirene, see: Dubai-Assibat, N.; Baceiredo, A.; Bertrand, G. *J. Am. Chem. Soc.* **1996**, *118*, 5216–5220.
- (20) Huisgen, R.; Sauer, J.; Seidel, M. *Justus Liebigs Ann. Chem.* **1962**, 654, 146.
- (21) Markgraf, J. H.; Brown, S. H.; Kaplinsky, M. W.; Peterson, R. C. *J. Org. Chem.* **1964**, *29*, 2629.
- (22) Scheiner, P. *J. Org. Chem.* **1969**, *34*, 199. Scheiner, P.; Dinda, J. F. Jr. *Tetrahedron* **1970**, *26*, 2619.
- (23) Wentrup, C.; Damerius, A.; Reichen, W. *J. Org. Chem.* **1978**, *43*, 2037. Wentrup, C.; Benedikt, J. *J. Org. Chem.* **1980**, *45*, 1407. See also: Muchall, H. M. *J. Phys. Chem. A* **2011**, *115*, 13694.
- (24) Gleiter, R.; Retting, W.; Wentrup, C. *Helv. Chim. Acta* **1974**, *57*, 2111.
- (25) Wentrup, C. *Helv. Chim. Acta* **1978**, *61*, 1755. Padwa, A.; Caruso, T.; Plache, D. *J. Chem. Soc., Chem. Commun.* **1980**, 1299. Padwa, A.; Caruso, T.; Nahm, S. *J. Org. Chem.* **1980**, *45*, 4065. Padwa, A.; Caruso, T.; Nahm, S.; Rodriguez, A. *J. Am. Chem. Soc.* **1982**, *104*, 2865.
- (26) Wong, M. W.; Leung-Toung, R.; Wentrup, C. *J. Am. Chem. Soc.* **1993**, *115*, 2465.
- (27) (a) Schissel, P.; Kent, M. E.; McAdoo, D. J.; Hedaya, E. *J. Am. Chem. Soc.* **1970**, *92*, 2147. (b) Wentrup, C.; Wilczek, K. *Helv. Chim. Acta* **1970**, *53*, 1459. (c) Wentrup, C.; Wentrup-Byrne, E.; Muller, P. *J. Chem. Soc., Chem. Commun.* **1977**, 210. (d) Wentrup, C. *Top. Curr. Chem.* **1976**, 173.
- (28) Wong, M. W. *Chem. Phys. Lett.* **1996**, *256*, 391.
- (29) Kurzer, F.; Douraghi-Zadeh, K. *Chem. Rev.* **1967**, *67*, 107.
- (30) McMahon, R. J.; Abelt, C. J.; Chapman, O. L.; Johnson, J. W.; Kreil, C. L.; LeRoux, J.-P.; Mooring, A. M.; West, P. R. *J. Am. Chem. Soc.* **1987**, *109*, 2456.
- (31) Dunkin, I. R. *Matrix-Isolation Techniques*; Oxford University Press: Oxford, 1998.
- (32) Duvernai, F.; Borget, F.; Aycard, J.-P. *J. Phys. Chem. A* **2005**, *109*, 603.
- (33) *N*-Phenyl-*N'*-(trimethylsilyl)carbodiimide **26**: Ruppert, I. *Tetrahedron Lett.* **1977**, 1987. Ruppert, I. *Angew. Chem., Int. Ed. Engl.* **1977**, *16*, 311. Itoh, K.; Okamura, K.; Ishii, Y. *J. Organomet. Chem.* **1974**, *65*, 327.
- (34) Wentrup, C.; Fischer, S.; Maquestiau, A.; Flammang, R. *Angew. Chem., Int. Ed. Engl.* **1985**, *24*, 56.
- (35) *C*-Methyl-*N*-(trimethylsilyl)nitrile imine **27**: IR (neat,  $-196\text{ }^{\circ}\text{C}/\text{cm}^{-1}$ , experimental wavenumbers with intensities *m*, *s*, vs followed by calculated anharmonic wavenumbers/intensities in parentheses (B3LYP/6-31G\*)) 2950 *s* (2988/34), 2259 *vs* (2283/432), 1440 *m* (1424/81), 1365 *m* (1388/311), 1290 *s* (1294/20), 875 *s* (899/251), 835 *s* (855/25), 755 *m* (775/33), 740 *m* (761/22). This compound rearranged to *N*-phenyl-*N'*-(trimethylsilyl)carbodiimide (2185  $\text{cm}^{-1}$ ) on photolysis of the film at 254 or 303 nm.
- (36) Meier, H.; Heinzelmann, W.; Heimgartner, H. *Chimia* **1980**, *34*, 504.
- (37) Hayes, J. C.; Sheridan, R. S. *J. Am. Chem. Soc.* **1990**, *112*, 5881.
- (38) Chapman, O. L.; LeRoux, J.-P. *J. Am. Chem. Soc.* **1978**, *100*, 282. Chapman, O. L.; Sheridan, R. S.; LeRoux, J.-P. *J. Am. Chem. Soc.* **1978**, *100*, 6245.
- (39) Wentrup, C.; Maquestiau, A.; Flammang, R. *Org. Mass. Spectrom.* **1981**, *16*, 115.
- (40) Réau, R.; Veneziani, G.; Dahan, F.; Bertrand, G. *Angew. Chem., Int. Ed. Engl.* **1992**, *31*, 439.
- (41) Authentic triphenylmethyl cyanide was synthesized according to a literature method: Budde, W. M.; Potempa, S. *J. Am. Chem. Soc.* **1952**, *74*, 258.
- (42) (a) Arthur, M. P.; Goodwin, H.; Baceiredo, A.; Dillon, K. B.; Bertrand, G. *Organometallics* **1991**, *10*, 3205. (b) Arthur, M. P.; Baceiredo, A.; Bertrand, G. *J. Am. Chem. Soc.* **1991**, *113*, 5856 (IR (ether) 2160  $\text{cm}^{-1}$ ).
- (43) Qiao, G. G.; Andraos, J.; Wentrup, C. *J. Am. Chem. Soc.* **1996**, *118*, 5634.
- (44) Frisch, M. J. et al. *Gaussian 09*, Revision A.2; Gaussian, Inc.: Wallingford, CT, 2009.
- (45) Bégué, D.; Gohaud, N.; Pouchan, C.; Lievin, J.; Cassam-Chenai, P. *J. Chem. Phys.* **2007**, *127*, 164115.
- (46) Gohaud, N.; Bégué, D.; Darrigan, C.; Pouchan, C. *J. Comput. Chem.* **2005**, *26*, 743.

- (47) Bégué, D.; Baraille, I.; Garrain, P. A.; Dargelos, A.; Tassaing, T. *J. Chem. Phys.* **2010**, *133*, 034102.
- (48) Gohaud, N.; Bégué, D.; Pouchan, C. *Int. J. Quantum Chem.* **2005**, *104*, 773.
- (49) Kawauchi, S.; Tachibana, A.; Mori, M.; Shibusa, Y.; Yamabe, T. *J. Mol. Struct. (Theochem)* **1994**, *310*, 255.
- (50) Wentrup, C.; Blanch, R.; Briehl, H.; Gross, G. *J. Am. Chem. Soc.* **1988**, *110*, 1874. Kvaskoff, D.; Bednarek, P.; George, L.; Pankajakshan, S.; Wentrup, C. *J. Org. Chem.* **2005**, *70*, 7947.